

STRUCTURE OF AN EVAPORATING FLOW  
INSIDE A HEATED POROUS METAL

V. A. Maiorov and L. L. Vasil'ev

UDC 532.685:536.24

Results are presented from an experimental study of the structure of an effluent two-phase flow and the temperature field on the external surface of a porous metal, with volume heat release during evaporative cooling by the liquid.

Organizing the evaporation of a flow of heat carrier inside heated porous metals permits maximization of the rate of heat transfer, particularly under special conditions such as in the presence of critical parameters or weightlessness — when the vapor film formed at the heat-transfer surface creates a high thermal resistance. In constructing a correct analytical model of the process, experimental data on the structure of an evaporating flow in porous metals is of particular value. The generalization of available results on these questions performed in [1] showed that information on the most important features of the process is lacking.

Presented below are results of an experimental study of the temperature field of the external surface of a porous metal with volume heat release during cooling by the evaporating flow of heat carrier inside it. Also presented are results of visual observations and photographs of the discharge of the flow.

The experiment performed involved the distilled-water cooling of porous specimens heated by a direct electrical current. The specimens, rectangular beams  $10 \times 16 \times 125$  mm, were made of 63-100- $\mu\text{m}$  dendritic particles of stainless-steel Kh17N2 powder. The porosity of the specimens was 0.24-0.38. Figure 1 shows a specimen prepared for testing. The specimen 1 is butt-joined by soldering to current-conducting copper buses 2. A poronite strip 3 is glued to the side of the specimen to attach and lead out the thermoelectrode conductors. A ruler is installed on the strip close to the outer surface. The specimen is equipped with 24 Chromel-Copel thermocouples. The experimental unit makes it possible to smoothly vary the power delivered to the specimen and the flow of heat carrier (coolant). The coolant in this case was distilled water, carefully deaerated and filtered. A similar experimental unit was described in [2].

The mean volume heat release  $q_v$  was calculated from the power supplied to the specimen and embraced a range  $q_v = (0.5-14) \cdot 10^7$  W/m<sup>3</sup> in the tests. The unit flow rate of the water changed within the range  $G = 0.040-0.65$  kg/m<sup>2</sup>·sec. Considerable difficulties are encountered in measuring the temperature of the outer surface of a porous specimen heated by a direct current. The specimen is porous, and the thermocouple cannot be installed in a groove. The direct electrical current may cause serious distortions in the measured thermal emf due to voltage jumps. Finally, the effluent two-phase flow intensively cools the soldered joint.

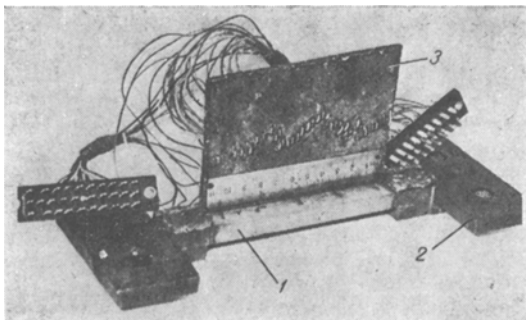


Fig. 1. General view of specimen, ready for the experiment.

Novolipetsk Polytechnic Institute. A. V. Lykov ITMO, Academy of Sciences of the Belorussian SSR, Minsk. Translated from *Inzhenerno-Fizicheskii Zhurnal*, Vol. 41, No. 6, pp. 965-969, December, 1981. Original article submitted December 31, 1980.

TABLE 1. Parameters of Evaporative Liquid Cooling of Porous Specimens ( $t_1$ - $t_5$ , °C)

Frame in Fig. 2	$q_v \cdot 10^{-7}$ , W/m <sup>3</sup>	G, kg/m <sup>2</sup> ·sec	$t_1$	$t_2$	$t_3$	$t_4$	$t_5$
a	0	0	20	20	20	20	20
b	2,27	0,158	100	99	98	100	99
c	3,43	0,174	99	99	98	100	99
d	6,67	0,238	99	100	99	340	324
e	10,30	0,650	100	98	99	100	99

A special technology was developed to make and attach the thermocouples. First one thermoelectrode 0.15-mm diameter is attached by electrostatic welding to the specimen surface. A second thermoelectrode is then attached on top of the first at the point where the latter contacts with the specimen surface.

Table 1 shows parameters of the test regimes. Figure 2 shows photographs of the most characteristic patterns of discharge of the evaporating flow from the specimen. The porous specimen was installed with its outer surface horizontally downward, so that the outflowing liquid phase would not accumulate on the surface and distort the flow pattern. The photographs were taken from below, and the drops of liquid visible in Fig. 2d and e are falling. Part of the ruler is visible at the bottom of the frames in Fig. 2a and c-e and the numbers on the scale, inverted in Fig. 1, are in the upright position.

Figure 2a shows photographs of the dry outer surface of the specimen before the experiment. The temperatures  $t_1$ - $t_5$  were measured with thermocouples 1-5 welded to the specimen surface. Five other thermocouples were attached about 2 mm away to measure the temperature of the effluent flow. The latter thermocouples are nearly indistinct from the first row of thermocouples in Fig. 2a but may be distinguished by the conductors leading from the poronite strip.

The pattern of discharge of the evaporating flow depends on the level of heat release. Three ranges of heat release  $q_v$  were noted for the specimens: up to  $3 \cdot 10^7$  W/m<sup>3</sup>, from 3 to  $6 \cdot 10^7$  W/m<sup>3</sup>, and above  $6 \cdot 10^7$  W/m<sup>3</sup>. The transition from single-phase efflux of the water to a regime of complete evaporation of the flow is assured within each of these ranges by an increase in heat release at a constant flow rate or a decrease in flow rate at a constant heat release. Figure 2 shows the most typical patterns observed in each of the heat-release ranges.

At a volume heat-release level  $q_v < 3 \cdot 10^7$  W/m<sup>3</sup>, hemispherical domes of 2-3-mm diameter with a thin sheath are formed on the outer surface, which is covered with a film of the liquid. The destruction of these domes is accompanied by the spraying of microdrops. The thickness of the film then gradually decreases. The dimensions of the domes decrease as well, but their density and the frequency of their appearance increase. Here, domes are formed at the same sites above vapor sources in the pores. The change in the dimensions and frequency of appearance of such domes on the specimen surface, the result of the lengthwise nonuniformity of the surface, is evident in Fig. 2b. The dimensions of the domes decrease going from the first to the fifth thermocouple. The liquid film then disappears from the specimen surface and the latter becomes dark and moist, then dry. The surface of most of the specimens dries evenly, with the drying spreading rapidly over the entire surface.

With a volume heat release  $q_v = (3-5) \cdot 10^7$  W/m<sup>3</sup>, small chains of tiny vapor-air bubbles can be seen emanating from the pores before visible boiling of the liquid in the flow. The velocity of the bubbles in these chains increases with an increase in heat release, and the bubbles burst on the surface of the film, creating fine ripples in the latter. The bubble chains subsequently merge and form continuous vapor microstreams issuing from pores in the material. These streams permeate the entire film and are visible underneath it as small white dots covering the entire surface of the specimen. The number and intensity of these streams increase as heat release increases. This is accompanied by noise, which gradually increases as well. Moving white emulsion build-ups appear on the surface of the film (Fig. 2c). If the specimen is uniformly permeable, these build-ups become less mobile as the liquid film becomes thinner and acquire a fine foamlike structure. The specimen surface dries, and three zones become evident: dry surface; surface covered with accumulations of the fine foam structure; an intermediate (between the first two zones) zone of dark moist

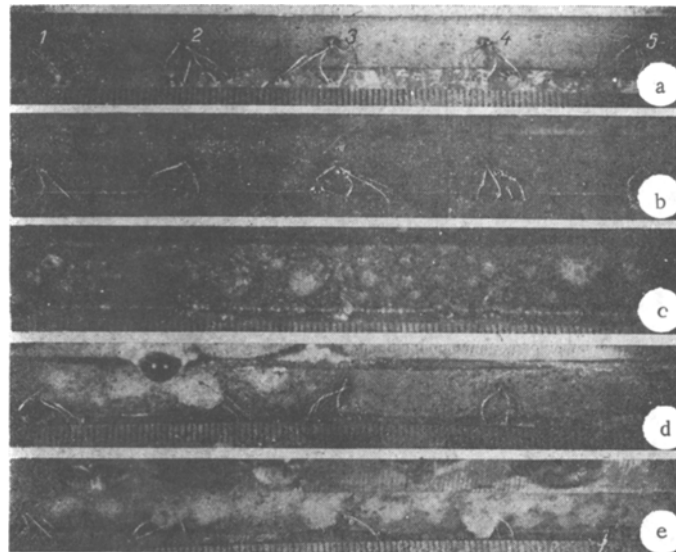


Fig. 2. Change in structure of evaporating flow of water leaving porous specimen as volume heat release intensifies (explanations in text and table).

surface with a gradually varying liquid saturation. Under these conditions, we see the outflow of moist vapor, with fine microdroplets in the form of a mist, from the dark moist surface. The flow of superheated steam from the dry part of the surface contains no mist. However, at such a level of heat release, most of the investigated specimens are characterized by local drying of their surface followed by a gradual increase in the fraction of dry surface as heat release increases. Here, a sharp boundary is seen between the dry surface and the surface covered with the liquid film permeated with vapor microstreams. In Fig. 2d, the boundary is located next to the third thermocouple. To the left is the liquid film permeated by white vapor microstreams which form the emulsion build-ups. To the right of the third thermocouple is the dry surface. It should be noted that the temperature of the outer surface of the specimen opposite the dry part of the surface remains below the saturation temperature.

With a volume heat release  $q_v > 6 \cdot 10^7 \text{ W/m}^3$ , the number of vapor microstreams increases and the intensity of their discharge is so great that individual microstreams cannot be distinguished. The liquid film on the specimen surface, permeated by innumerable vapor microstreams, swells and becomes a white emulsion with a large quantity of mobile build-ups (Fig. 2e). A loud noise is audible. In some cases the surface is dried to the point where the liquid film disappears and two zones are formed on the surface: a dry zone, and a dark moist zone with small fine-structured accumulations of foam. For most of the specimens, drying occurs with the presence of a sharp boundary and a very hot dry part of the surface.

Analysis of the temperature fields of the external surface for the numerous available photographs of flow patterns (especially for those in Fig. 2) shows the following. At any of the investigated levels of heat release up to  $q_v = 14 \cdot 10^7 \text{ W/m}^3$ , the temperature of the outer surface, when a two-phase flow in any form is issuing from it, remains equal to the saturation temperature. The temperature of the dark moist surface is also equal to the saturation temperature for such conditions up to heat-release levels  $q_v = 10.7 \cdot 10^7 \text{ W/m}^3$ .

The above data permits the following conclusion: the rate of intrapore volume heat transfer in the evaporation of a flow of water in the investigated porous metals is so high that the temperature of the metal is nearly the same as the saturation temperature at heat-release levels up to  $q_v = 1.07 \cdot 10^8 \text{ W/m}^3$ , with complete evaporation of the flow.

Thus, we observed in observing on the outer surface of a porous specimen the complete change of structure of an outgoing two-phase flow — from the appearance of small chains of tiny gas-vapor bubbles to drying of the surface. It is quite obvious that it is impossible to obtain information on the change in the structure of the flow as it evaporated inside

this porous material. At the same time, the outer surface of the specimen — with the changing patterns of two-phase flow — represents a succession of sections of the specimen through its thickness which permits visual observation of the smooth change in the structure of the flow. Thus, on the basis of the above patterns of efflux of a two-phase evaporating flow from a porous metal under different conditions, the mechanism and structure of the evaporating flow inside the heated porous metal may be represented as follows. Small vapor bubbles are formed at the beginning of the evaporation region at individual centers. These bubbles fill the entire cross section of a given pore. The vapor bursts through the largest pore-connected channels and flows in individual microstreams. Sections of these vapor microstreams are intercepted and captured by plugs of liquid.

Both the number of vapor-formation centers and the number of vapor microstreams increase as the flow moves, and the streams gradually fill all of the smaller pore channels. The liquid plugs are spread out and thinned. Here, most of the liquid moves in the form of a gradually thinning microfilm which envelops particles of the metal and fills individual dead-end pores. The velocity of the vapor is continuously increasing. Due to the sharp construction and curvature of the channels and the breakthrough of vapor accompanying bubble formation in pores that were previously filled with liquid, fine liquid bridges are continuously formed and destroyed. The microfilm of liquid on the walls of the channels then gradually dries and the liquid bridges collapse into fine microdrops. Due to a sharp change in the direction of motion in the curved channels, the microdrops strike the surface, are caught by semiopen pores, adhere, and are evaporated — evaporation of the flow is completed.

#### LITERATURE CITED

1. V. A. Maiorov and L. L. Vasil'ev, "Heat exchange and stability in the motion of a coolant evaporating in porous metal-ceramic materials," *Inzh. Fiz. Zh.*, 36, No. 5, 914-134 (1979).
2. V. A. Maiorov, "Unit for investigating heat exchange and resistance in the evaporative cooling of a porous heat-releasing element," in: *Low-Temperature Heat Tubes and Porous Heat Exchangers* [in Russian], A. V. Lykov ITMO Akad. Nauk Belorussian SSR, Minsk (1977), pp. 38-48.